12WCEE 2000

MODELING THE GROUND MOTION DURING THE 1995 HYOGO-KEN NANBU EARTHQUAKE BY A 3-D BEM

Shojiro KATAOKA[1]

SUMMARY

The 1995 Hyogo-ken Nanbu earthquake caused serious damage in and around Kobe City. In particular, heavily damaged buildings and houses were concentrated in a narrow zone, so-called "earthquake disaster belt", which was designated as seismic intensity 7 on JMA scale. In this study, ground motion in Kobe area that was excited by faulting is simulated by a 3-D direct BEM using an irregularly layered ground model and a source model. Then the synthetic ground motions are compared with the observed ones to discuss the validity of the simulation.

INTRODUCTION

The 1995 Hyogo-ken Nanbu earthquake (M7.2) took a heavy toll of lives and caused great property damage in cities near its focal region, especially in Kobe City. Many lifeline structures such as highway bridges also collapsed and indicated that ground motion during the earthquake was extremely strong. Based on investigation of damage degrees, a narrow zone of about 1km wide was designated as the seismic intensity 7 on JMA scale and called "earthquake disaster belt".

After the earthquake, we have realized more strongly than ever that the prediction of strong ground motion caused by future large earthquakes is important to prevent such serious disaster. Since the prediction requires simulation methods of near-field ground motion, they should be more sophisticated and incorporated into seismic design procedures. In this study, a 3-D boundary element method (BEM) is employed to simulate the ground motion in the Kobe area that was excited by faulting of the 1995 Hyogo-ken Nanbu earthquake.

3-D BEM FOR GROUND MOTION SIMULATIONS

Let us consider irregularly layered media in which seismic wave generated by faulting is incident. Seismic wave propagated in such media has been well idealized and computed by boundary element method (BEM) [e.g., Kobayashi and Nishimura, 1982; Kawase, 1988). An outline of the method used in this study, a 3-D direct

BEM in frequency domain, is presented in this section. A two-layered linear isotropic homogeneous medium that consists of a subsurface and a basement layers is considered.

Boundary Integral Equations:

A boundary integral equation on the boundary of layer A, the subsurface layer, in x_1-x_2-x_3 Cartesian coordinate can be written as

$$c_{ij}(\boldsymbol{x})u_j(\boldsymbol{x}) + \int_{G_A} T_{ij}(\boldsymbol{x},\boldsymbol{y})u_j(\boldsymbol{y})dG(\boldsymbol{y}) - \int_{G_A} U_{ij}(\boldsymbol{x},\boldsymbol{y})t_j(\boldsymbol{y})dG(\boldsymbol{y}) = 0 \qquad (1)$$

where u_i and t_i denote x_i-component of the displacement and traction, G_A the boundary of layer A, U_{ij} the fundamental solution, T_{ij} its traction, $\boldsymbol{y}$ and $\boldsymbol{x}$ source and field points, respectively, and c_{ij} a free-term which depends on the boundary shape at $\boldsymbol{x}$. The first integral on the left-hand side is to be interpreted in the sense of

[1] *Ground Vibration Div, Public Works Research Institute, Ministry of Construction, Tsukuba, Japan Email:s-katao@pwri.go.jp*

Cauchy principal value.
Similarly, a boundary integral equation on the boundary of layer *B*, the basement layer that is assumed to include fault sources, can be written as (Niwa *et al*., 1986)

$$c_{ij}(\boldsymbol{x})u_j(\boldsymbol{x}) + \int_{G_B} T_{ij}(\boldsymbol{x},\boldsymbol{y})u_j(\boldsymbol{y})dG(\boldsymbol{y}) - \int_{G_B} U_{ij}(\boldsymbol{x},\boldsymbol{y})t_j(\boldsymbol{y})dG(\boldsymbol{y}) = y_i(\boldsymbol{x}) \quad (2)$$

where G_B denotes the boundary of layer *B* and y_i represents effects of the incident wave.

If a point dislocation source locating at $\boldsymbol{y}$ is considered, y_i is expressed as

$$y_i(\boldsymbol{x}) = T_{ij}(\boldsymbol{x},\boldsymbol{y})d_j(\boldsymbol{y}) \quad (3)$$

where $d_j = u_j^+ - u_j^-$ denotes x_j-component of the dislocation.

Matrix Equations and Boundary Conditions:

By discretizing the boundaries into a set of boundary elements, Eqs. (2) and (3) can be written in a matrix form as (Brebbia *et al*., 1984)

$$\boldsymbol{H}_A\boldsymbol{u}_A - \boldsymbol{G}_A\boldsymbol{t}_A = \boldsymbol{0}$$
$$\boldsymbol{H}_B\boldsymbol{u}_B - \boldsymbol{G}_B\boldsymbol{t}_B = \boldsymbol{y} \quad (4)$$

where $\boldsymbol{u}$ and $\boldsymbol{t}$ are the nodal displacement and nodal traction vectors, respectively. $\boldsymbol{y}$ is a vector of which components are y_i. The subscripts of the matrices and vectors denote the layer (*A* or *B*) which they belong to.

In this paper, isoparametric linear elements are adopted to discretize boundaries. Strongly singular integrals, which are required to calculate diagonal components of $\boldsymbol{H}$, and free-terms are directly evaluated referring to recent studies [Guiggiani and Gigante, 1990; Mantic, 1993].
Continuity and equilibrium conditions along the boundary between the layers A and B require that

$$\boldsymbol{u}_A = \boldsymbol{u}_B$$
$$\boldsymbol{t}_A + \boldsymbol{t}_B = \boldsymbol{0} \quad (5)$$

Solving Eqs. (4) and (5) simultaneously carries out ground motion simulations by the 3-D BEM.

SOURCE AND GROUND MODELS

Source Model:

The source model determined by Wald [Wald, 1996] is used in the simulation. However, the southwest portion of the fault (Nojima fault) is neglected because it is considered to have much less contribution to the ground motion in the area under consideration than the northeast portion of the fault (Rokko fault). The fault rupture is assumed to be propagated radially along the fault plane from the hypocenter at a constant velocity of 2.8 [km/s]. The Rokko fault plane whose length and width are 40 [km] and 20 [km], respectively, is divided into 96 subfaults and the rupture of each subfault is represented by 25 point dislocation sources to represent a smooth rupture process.

Ground Model:

A deep basement structure of the Osaka plain is estimated from the local free-air gravity anomalies [Inoue *et al*., 1998]. A two-layered ground model is constructed with boundary elements based on the estimated basement structure. The plan of the basement layer of the BE model is shown in Figure 1.

Grid spacings for the subsurface and the basement are about 0.6 km and 1.2 km, respectively. Table 1 shows the velocity, density, and Q-values of the two layers that are based on the velocity model that was assumed to determine the source model [Wald, 1996]. The density of the basement layer of the BE model, 2.7 [t/m^3], is consistent with the density of the basement rock of the Osaka plain, 2.66 [t/m^3], estimated by Inoue et al. [Inoue et al., 1998].

Table 1: Velocity, density, and Q-values of the subsurface and basement layers of the BE model.

	P wave velocity [km/s]	S wave velocity [km/s]	density [t/m^3]	Q_P	Q_S
Subsurface	2.5	1.0	2.1	60	20
Basement	6.0	3.5	2.7	600	300

COMPARISON BETWEEN OBSERVED AND SYNTHETIC MOTIONS

The computation was carried out for 0.0625-0.500 [Hz] with an increment of 0.0156 [Hz]. Figure 3 shows observed and synthetic ground motion velocities at 14 stations listed in Table 2. The observed waveforms are band-pass filtered so that they have the same frequency range as the synthetics. The locations of these stations are shown in Figure 1. The upper and lower boxes show the observed and synthetic ground motions, respectively, and the solid lines in the lower boxes are the synthetics obtained by the 3-D BEM simulation described in **2.** and **3.**, while the broken lines are those obtained by Hisada's method [Hisada, 1994; Hisada, 1995] using 1-D (horizontally layered) ground models with subsurface and basement layers. The thickness of the subsurface layers of 1-D ground models are set to be the depth of basement surface at each station shown in Table 2.

Table 2: Strong motion stations with their epicentral distances and depth of the basement surface. Stations are listed in order of epicentral distances.

abbreviation	station location	epicentral distance [km]	depth of basement surface [km]
(a) JMA	JMA Kobe station	18.2	0.12
(b) PIS	Port Island (GL -83m)	19.6	1.76
(c) FKA	Fukiai	21.0	1.13
(d) KBU	Kobe University	25.0	0.00
(e) RKI	Rokko Island	25.8	2.11
(f) SKH	Shin-Kobe substation	26.1	0.00
(g) MOT	Motoyama	28.2	0.89
(h) NKP	Nanko Power Plant	36.4	1.80
(i) AMA	Amagasaki	38.6	1.81
(j) SOG	Sogo Gijutsu Kenkyusho (GL -97m)	42.4	1.82
(k) FKS	Fukushima	43.4	1.87
(l) WOS	Nishi-Osaka	43.4	1.70
(m) ABN	Abeno	46.7	1.34
(n) OSA	JMA Osaka	48.9	0.82

In Figure 3 (a)-(g), the observed ground motions at stations in Kobe City, of which epicentral distances are less than 30 [km], are compared with the synthetics. Those observed and synthetic waveforms show a good agreement but the observed motions have amplitudes about 3 times as large as the synthetic motions. The difference can be explained by amplification due to shallower ground structure that is not modeled in the simulations. We can see small differences between the synthetic waveforms from the 3-D and 1-D simulations in (a)-(g) except that vertical ground motions of (b) and (c) are much more amplified by the 3-D ground structure.

Both the observed and synthetic waveforms of (a)-(g), especially (a), (d), and (f) where the subsurface is very thin, show shorter duration than those of (h)-(n). Long duration and waveforms of the observed ground motions of (k)-(n) are well reproduced by the 3-D BEM simulation rather than the 1-D simulation. This implies that it is better to take 3-D basement topography into account in ground motion simulations if it is obtained with accuracy as well as the Osaka plain.

CONCLUSIONS

To simulate near-field ground motion in irregularly layered media, a 3-D direct BEM was formulated, and then applied to a ground motion simulation of the 1995 Hyogo-ken Nanbu earthquake. We can find some agreement in duration and waveforms between the observed and the synthetic ground motions. However, since the

shallower ground structure is neglected in the simulation, the observed ground motions are not reproduced well especially in terms of amplitude.

ACKNOWLEDGEMENT

The authors greatly appreciate Prof. Nakagawa and Dr. Inoue of Osaka City University for offering the digital data of the depth of the basement rocks in the Osaka plain. We are also grateful to the Japanese Working Group on ESG and those who provided original data for distributing the source model and strong motion data used in this paper. The auto-mesh generation software is provided by Mr. K. Shiomi and Mr. H. Sasaki of Fujitu FIP Corporation. The computer code for the 1-D simulations used in this paper is the one coded by Prof. Hisada and open for academic use. The authors thank for their generosities.

REFERENCES

Brebbia, C. A., J. C. Tells and L. C. Wrobel (1984) *Boundary Element Techniques-Theory and Applications in Engineering*, Springer-Verlag.

Guiggiani, M. and A. Gigante (1990) "A general algorithm for multidimensional Cauchy principal value integrals in the boundary element method", *Trans. ASME*, 57, 906-915.

Hisada, Y (1994) "An efficient method for computing Green's functions for a layered half-space with sources and receivers at close depth", *Bull. Seism. Soc. Am.*, 84, 1456-1472.

Hisada, Y (1995) "An efficient method for computing Green's functions for a layered half-space with sources and receivers at close depth (Part 2)", *Bull. Seism. Soc. Am.*, 85, 1080-1093.

Inoue, N., K. Nakagawa and K. Ryoki (1998) "Gravity anomalies and basement structure in Osaka plain", *Butsuri-Tansa*, 51, 1-16 (in Japanese).

Kawase, H. (1988) "Time-domain response of a semi-circular canyon for incident SV, P, and Rayleigh waves calculated by the discrete wavenumber boundary element method", *Bull. Seism. Soc. Am.*, 78, 1415-1437.

Kobayashi, S. and N. Nishimura (1982) "Transient stress analysis of tunnels and cavities of arbitrary shape due to travelling waves", In P. K. Banerjee \& R. P. Shaw (eds.), *Developments in Boundary Element Methods -2*, Applied Science Publishers.

Mantic, V. (1993) "A new formula for the C-matrix in the Somigliana identity", *J. Elasticity*, 33, 191-201.

Niwa, Y., S. Hirose and M. Kitahara (1986) "Application of the boundary integral equation (BIE) method to transient response analysis of inclusions in a half-space", *Wave Motion*,8, 77-91.

Wald, D. J. (1996) "Slip history of the 1995 Kobe, Japan, earthquake determined from strong motion, teleseismic, and geodetic data", *J. Phys. Earth*, 44, 489-503

.

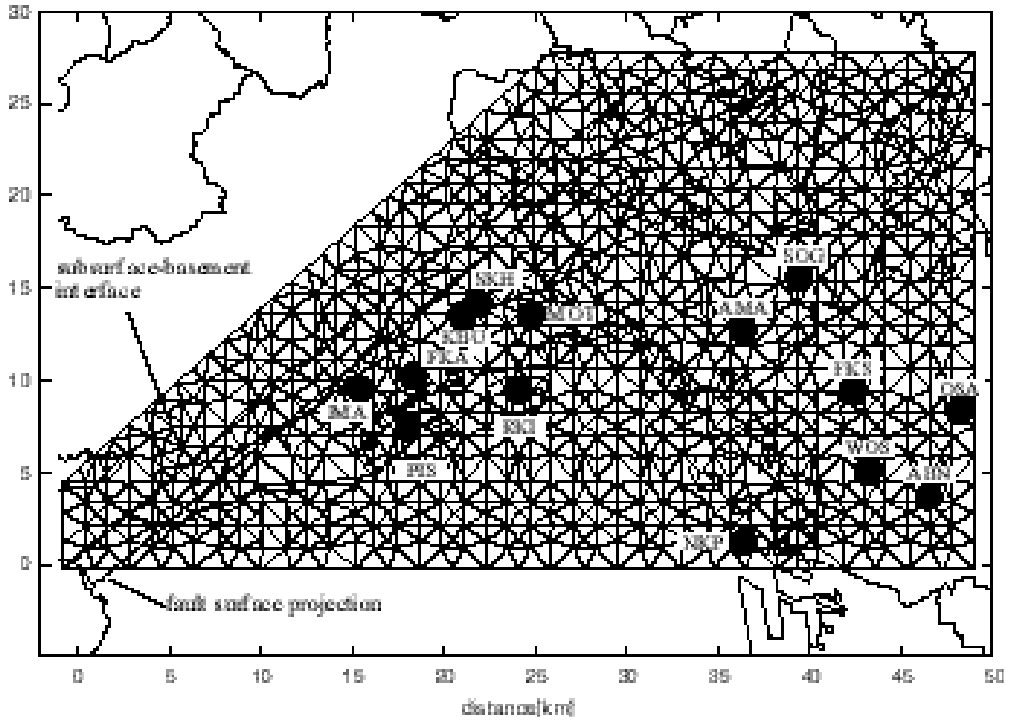

Figure 1: Plan of the BE model of the basement layer with strong motion stations. Observed ground motions recorded at these stations are compared with synthetic ground motions in Figure 3. The fault surface projection of the northeast portion of the source model proposed by Wald (1996) is also shown. The epicenter is at the origin (0, 0) of the coordinate system.

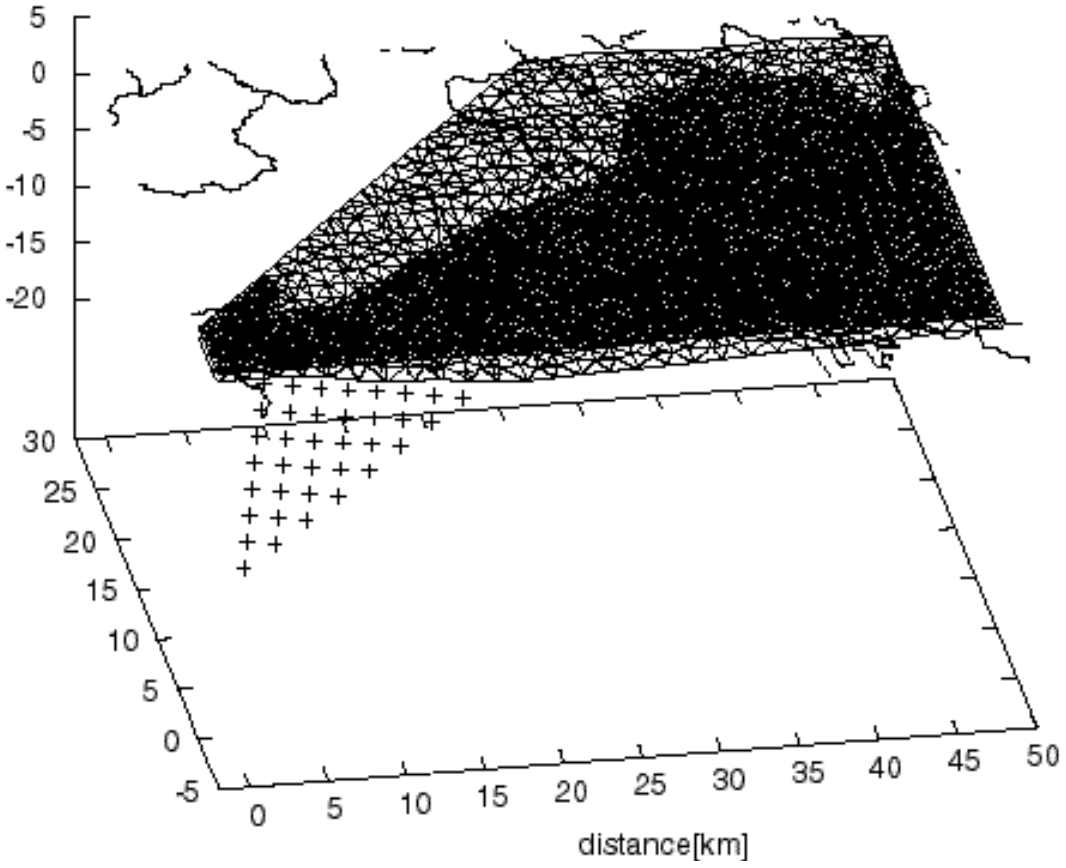

Figure 2: Perspective of the BE model with the centers of the subfaults (+). The hypocenter is at (0, 0, -17) of the coordinate system.

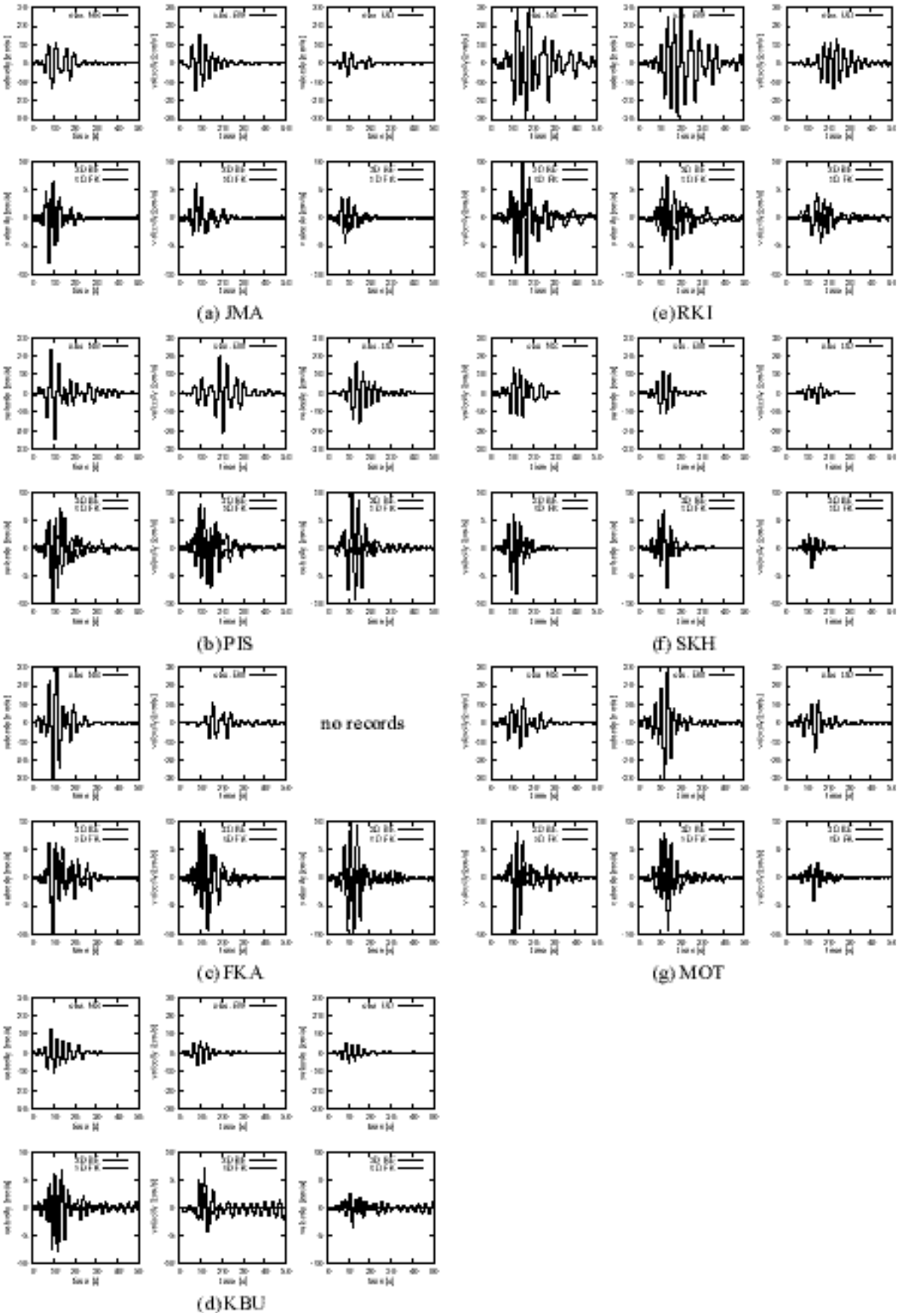

Figure 3: Comparison between the observed (upper boxes) and synthetic (lower boxes) ground motion velocities. The solid and broken lines in the lower boxes show the synthetics by the 3-D and 1-D simulations, respectively.

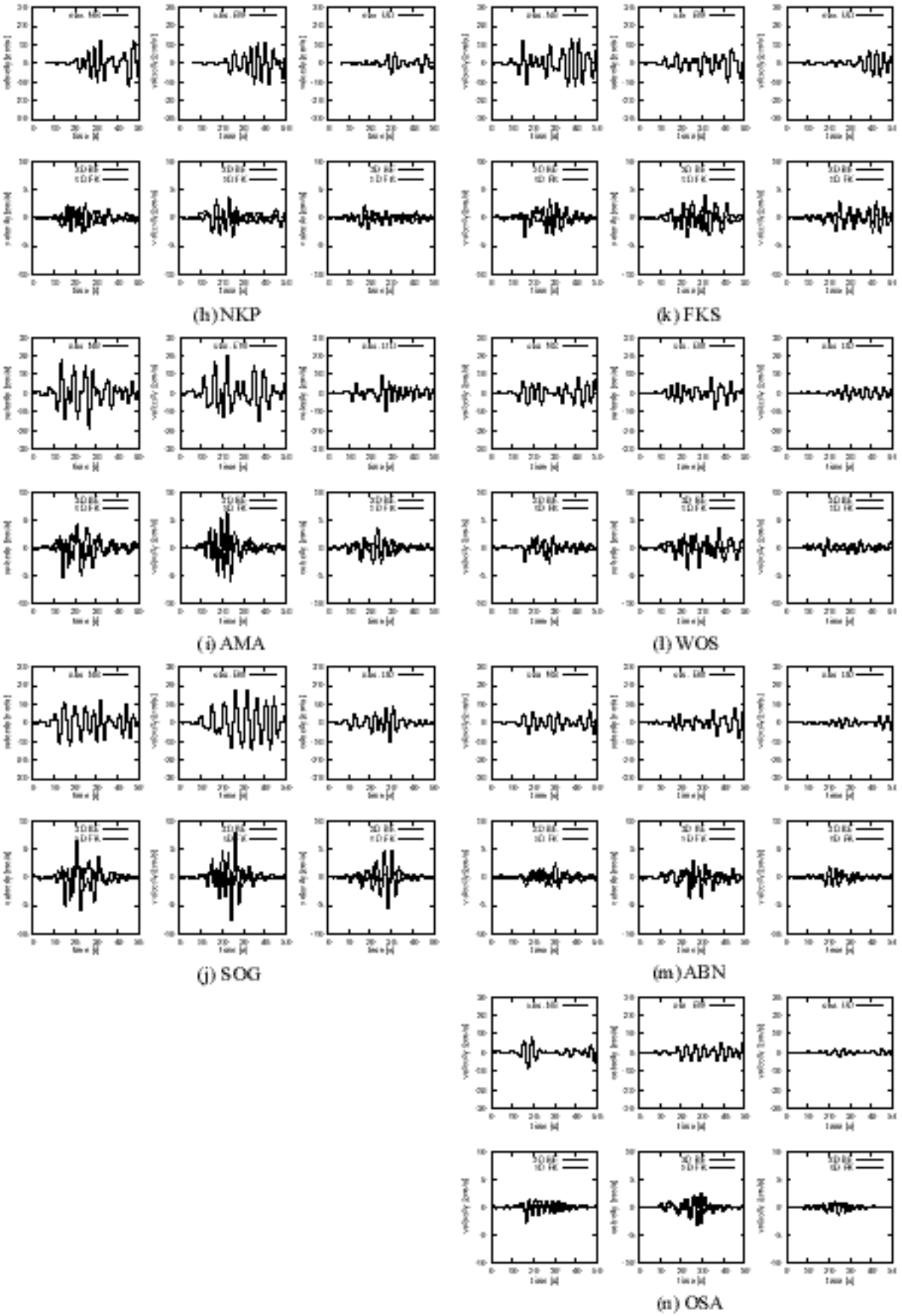

Figure 3 (cont.): Comparison between the observed (upper boxes) and synthetic (lower boxes) ground motion velocities. The solid and broken lines in the lower boxes show the synthetics by the 3-D and 1-D simulations, respectively.